



Supplement of

Characterization of a real-time tracer for isoprene epoxydiols-derived secondary organic aerosol (IEPOX-SOA) from aerosol mass spectrometer measurements

W. W. Hu et al.

Correspondence to: J. L. Jimenez (jose.jimenez@colorado.edu)

The copyright of individual parts of the supplement might differ from the CC-BY 3.0 licence.

Table S1. Pearson's correlation coefficients (R) between time series of organic ions and the PMF IEPOX-SOA factor for the SOAS study (SE US forest).

| Ion Formula | Ion mass | Correlation coefficient (R) |
|---|----------|-----------------------------|
| Ions with R > 0.8 | | |
| C ₅ H ₆ O ⁺ | 82.0419 | 0.97 |
| C ₅ H ₅ O ⁺ | 81.034 | 0.95 |
| C ₄ H ₅ ⁺ | 53.0391 | 0.90 |
| C ₄ H ₆ O ⁺ | 70.0419 | 0.88 |
| C ₃ H ₇ O ₂ ⁺ | 75.0446 | 0.87 |
| C ₃ H ₅ O ⁺ | 57.034 | 0.84 |
| C ₄ H ₆ ⁺ | 54.047 | 0.84 |
| CH ₃ O ⁺ | 31.0184 | 0.83 |
| C ₄ H ₇ O ₂ ⁺ | 87.0446 | 0.83 |
| C ₃ H ₆ ⁺ | 42.047 | 0.82 |
| C ₄ H ₂ ⁺ | 50.0157 | 0.82 |
| C ₅ H ₈ O ⁺ | 84.0575 | 0.82 |
| C ₄ H ₅ O ⁺ | 69.034 | 0.82 |
| C ₄ H ⁺ | 49.0078 | 0.82 |
| C ₃ H ₃ ⁺ | 39.0235 | 0.82 |
| C ₂ H ₃ ⁺ | 27.0235 | 0.81 |
| C ₃ H ⁺ | 37.0078 | 0.80 |
| C ₂ H ₅ ⁺ | 29.0391 | 0.80 |
| C ₄ H ₃ ⁺ | 51.0235 | 0.80 |
| C ₃ H ₂ ⁺ | 38.0157 | 0.80 |
| C ₃ H ₅ ⁺ | 41.0391 | 0.80 |
| CH ₂ O ⁺ | 30.0106 | 0.80 |
| Ions with lowest R | | |
| CHNO ⁺ | 43.0058 | -0.37 |
| CNO ⁺ | 41.998 | -0.12 |
| CN ⁺ | 26.0031 | -0.11 |
| Other common used ions in AMS | | |
| C ₂ H ₃ O ⁺ | 43.0184 | 0.72 |
| C ₃ H ₇ ⁺ | 43.0548 | 0.57 |
| CO ₂ ⁺ | 43.9898 | 0.66 |
| C ₃ H ₃ O ⁺ | 55.0184 | 0.72 |
| C ₄ H ₇ ⁺ | 55.0548 | 0.68 |
| C ₂ H ₄ O ₂ ⁺ | 60.0211 | 0.60 |

1
2
3

4 **Table S2.** Description of spectra which have higher $f_{C_5H_6O}$ than background $f_{C_5H_6O}$, labeled by
 5 number in Fig. 5.

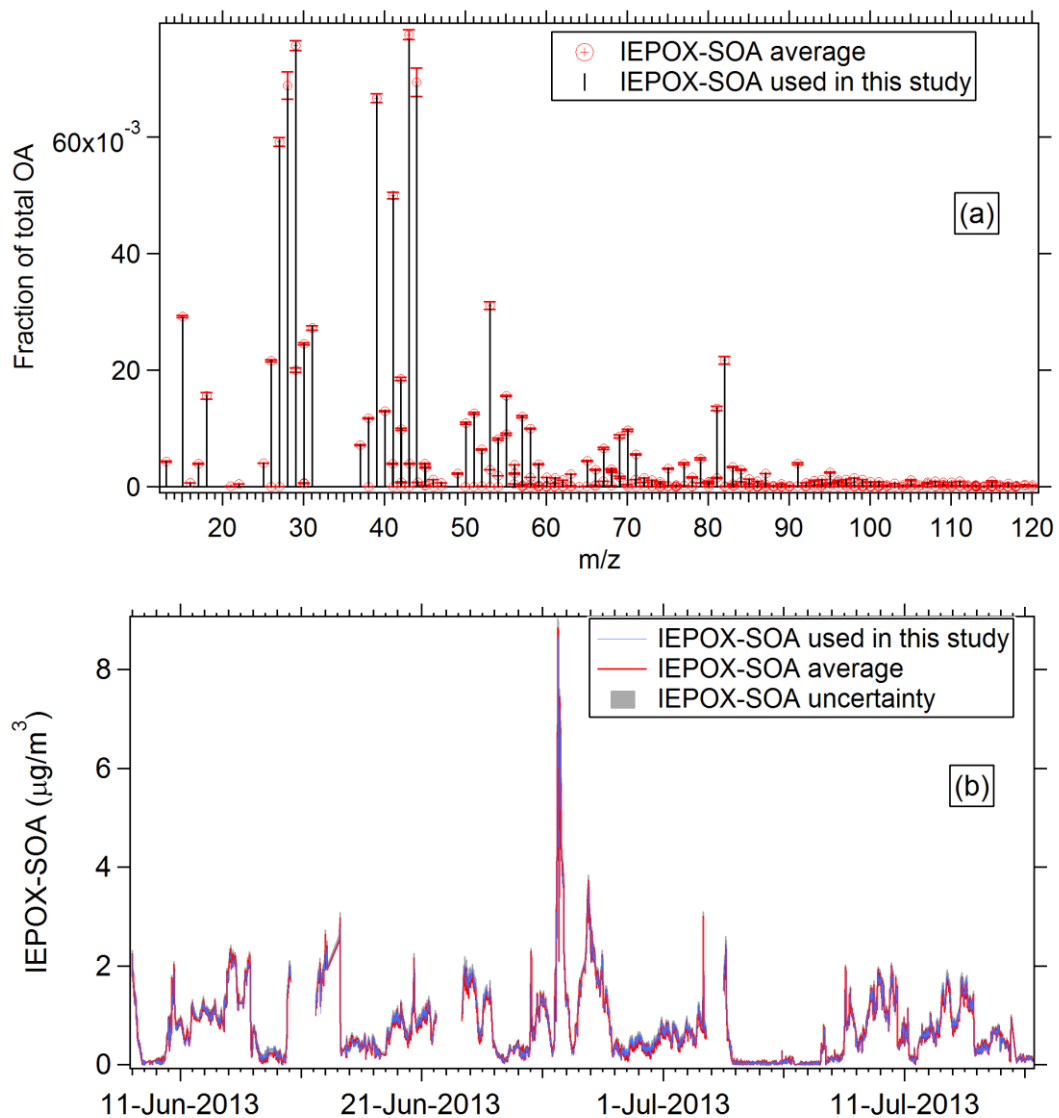
| Index | Spectra name | Description of spectra sources | References |
|-------|--|--|--|
| 1 | HOA ^a from CARES campaign | Isoprene emission influenced, aerosol is neutralized | (Setyan et al., 2012) |
| 2 | OA from CA Central Valley | Isoprene emission influenced, aerosol is slightly acidic. | (Dunlea et al., 2009) |
| 3 | NO ₃ + Δ-Carene reaction in Chamber | Biogenic SOA | Chamber study in CU |
| 4 | Ozonolysis α-terpene in Chamber | Biogenic SOA | (Chhabra et al., 2010) |
| 5 | SV-OOA ^b from SOAR | Slight biogenic influence | (Docherty et al., 2011) |
| 6 | SV-OOA from Paris summer campaign | Not mentioned in study, however, forests around the sampling site. | (Crippa et al., 2013) |
| 7 | NO ₃ + Δ-Carene reaction in Chamber | Biogenic SOA | Chamber study in CU |
| 8 | SV-OOA from SOAS | Isoprene and monoterpene influenced | This study |
| | NO ₃ + Δ-Carene reaction in Chamber | Biogenic SOA | Chamber study in CU |
| 10 | MO-OOA ^c in CARES campaign | Urban SOA with isoprene emission-influenced | (Setyan et al., 2012) |
| 11 | SV-OOA in MILAGRO | Urban SOA | (Aiken et al., 2009; Ulbrich et al., 2009) |
| 12 | LV-OOA in Paris summer | Urban-background SOA, forests around the sampling site. | (Crippa et al., 2013) |
| 13 | Adipic acid | Pure chemical OA standards | (Canagaratna et al., 2015) |
| 14 | 3-Hydroxy-3-Methylglutaric Acid | Pure chemical OA standards | (Canagaratna et al., 2015) |
| 15 | 4-ketopimelic acid | Pure chemical OA standards | (Canagaratna et al., 2015) |
| 16 | 5-Oxoazelaic acid | Pure chemical OA standards | (Canagaratna et al., 2015) |
| 17 | Gamma ketopimelic acid dilactone | Pure chemical OA standards | (Canagaratna et al., 2015) |

6 ^aHOA=Hydrocarbon-like OA

7 ^bSV-OOA=Semi-volatile oxygenated OA

8 ^cMO-OOA=More-oxidized oxygenated OA

9

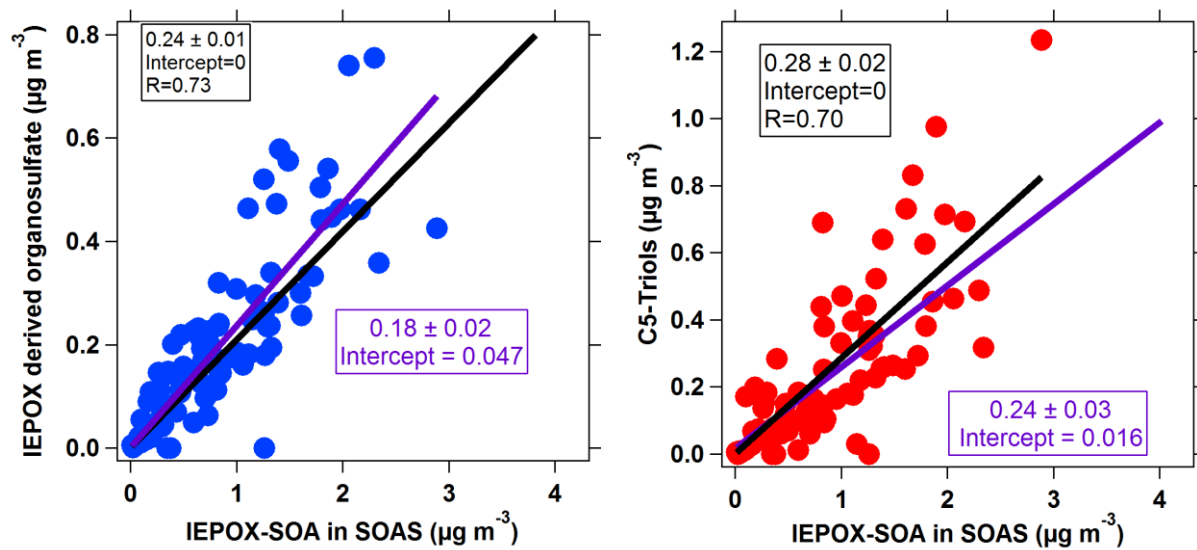


10

11 **Figure S1.** Results from bootstrapping analysis of the 4-factor solution of the SOAS dataset.
 12 Average IEPOX-SOA, with standard deviation, are shown for IEPOX-SOA (a) mass spectrum
 13 and (b) time series.

14

15

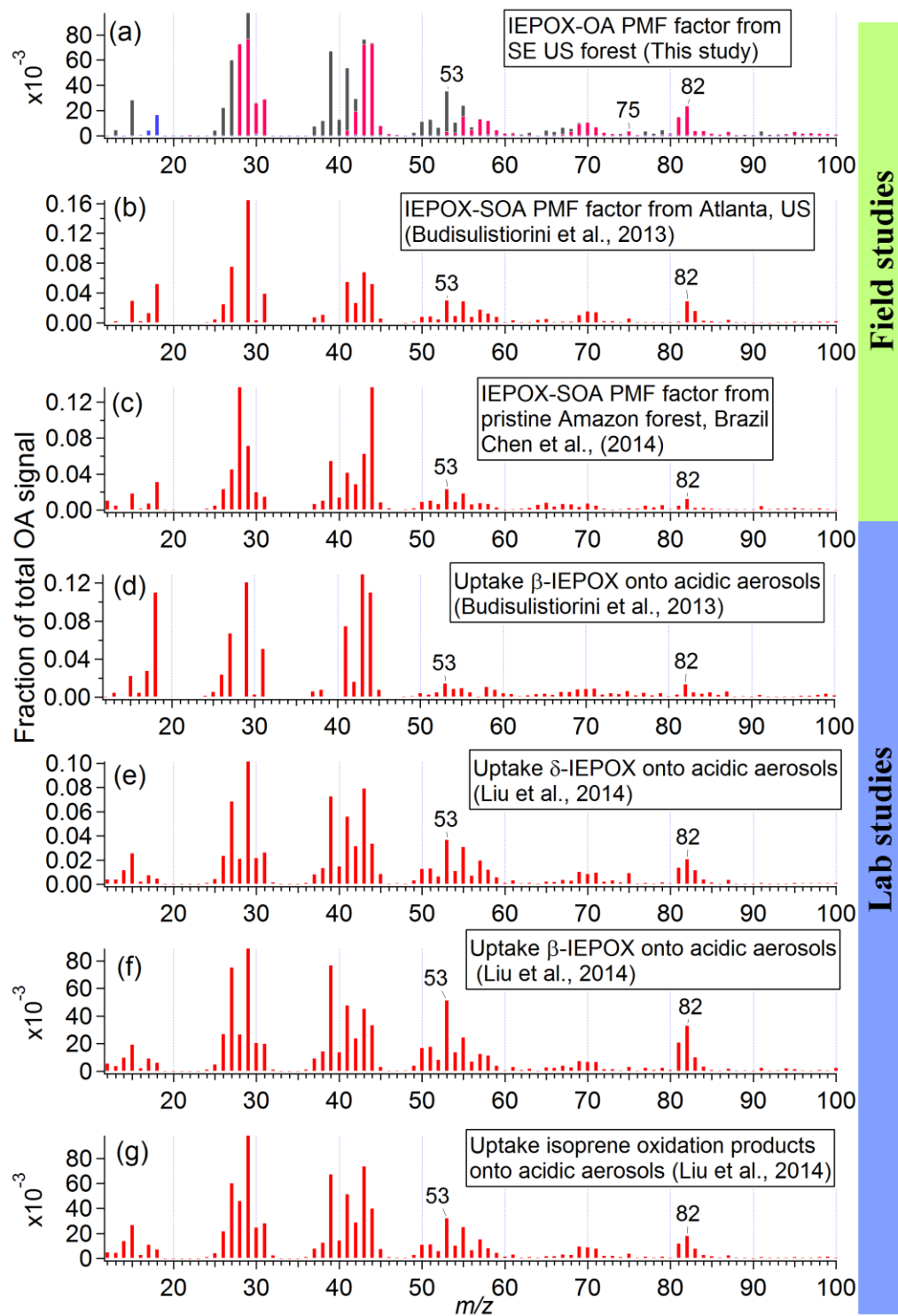


16

17 **Figure S2.** Scatter plots between IEPOX-derived organosulfate and C5-triols vs IEPOX-SOA_{PMF}
 18 in the SOAS study. The IEPOX-derived organosulfate and C5-triols were measured in GC/MS
 19 and LC/MS analysis of filter extracts (Lin et al., 2014; Budisulistiorini et al., 2015).

20

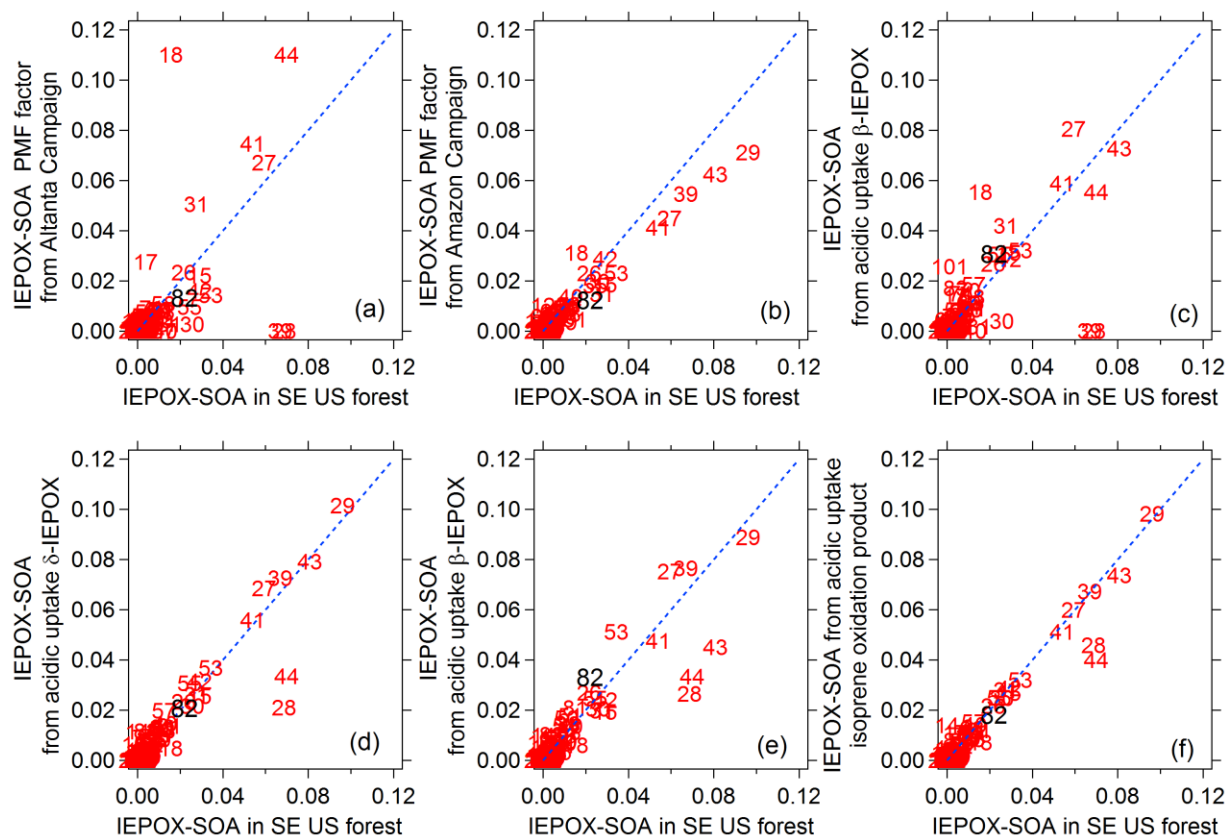
21



22

23 **Figure S3.** Mass spectra of IEPOX-SOA from different studies. Panel (a) – (c) are the results
 24 from field studies. Panel (d) – (g) are the results from lab studies.

25



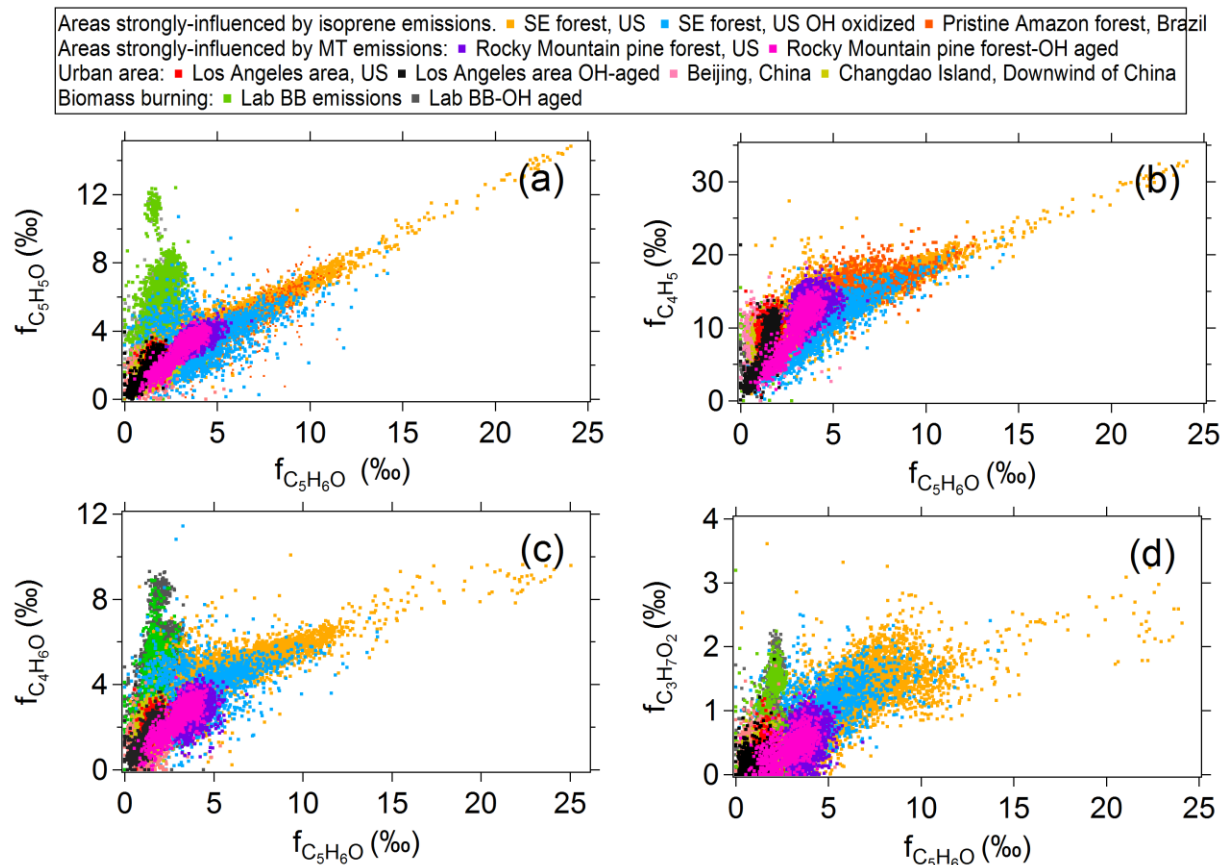
27

28 **Figure S4.** Scatter plots of IEPOX-SOA spectra in other studies vs IEPOX-SOA spectrum from
 29 this study (SOAS, SE US forest). The spectra on the y-axes are in the same order as Figures S1
 30 (b) to (g).

31

32

33

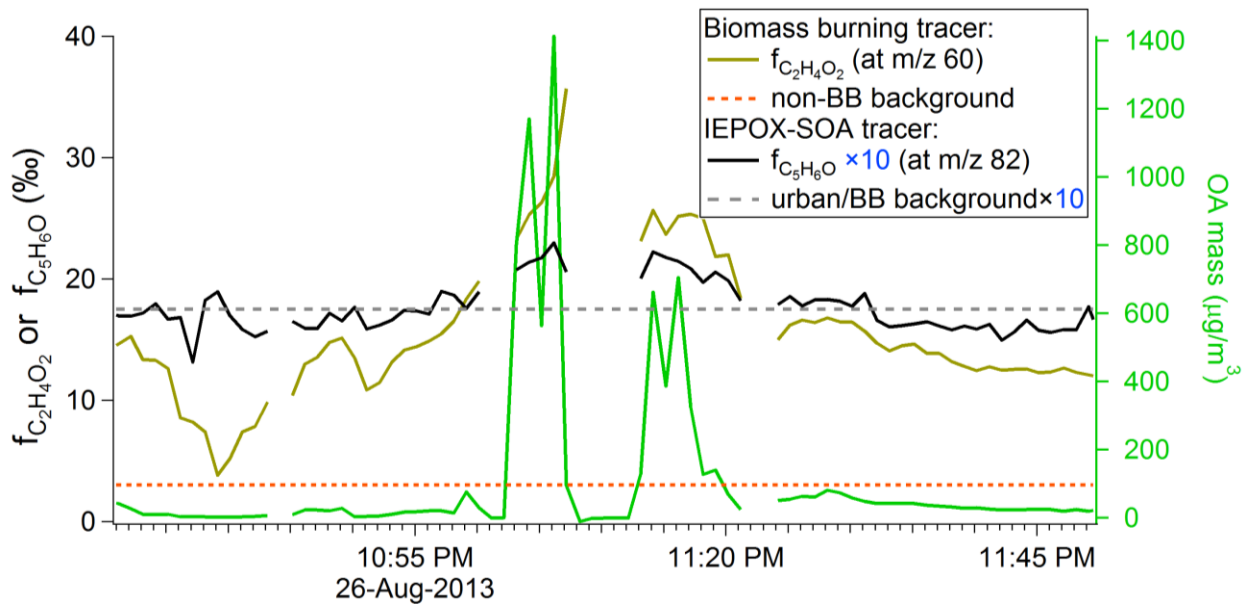


34

35 **Figure S5.** Scatter plots of abundance of ions versus $f_{C_5H_6O}^{OA}$ obtained in different studies: (a)
36 $f_{C_5H_5O}^{OA}$, (b) $f_{C_4H_5}^{OA}$, (c) $f_{C_4H_6O}^{OA}$, and (d) $f_{C_3H_7O_2}^{OA}$. Compared to $f_{C_5H_6O}^{OA}$, $f_{C_4H_5}^{OA}$, $f_{C_4H_6O}^{OA}$, and $f_{C_5H_5O}^{OA}$ have
37 high background levels in urban and biomass-burning emissions. The signal to noise of
38 $f_{C_3H_7O_2}^{OA}$ measured in AMS is very low.

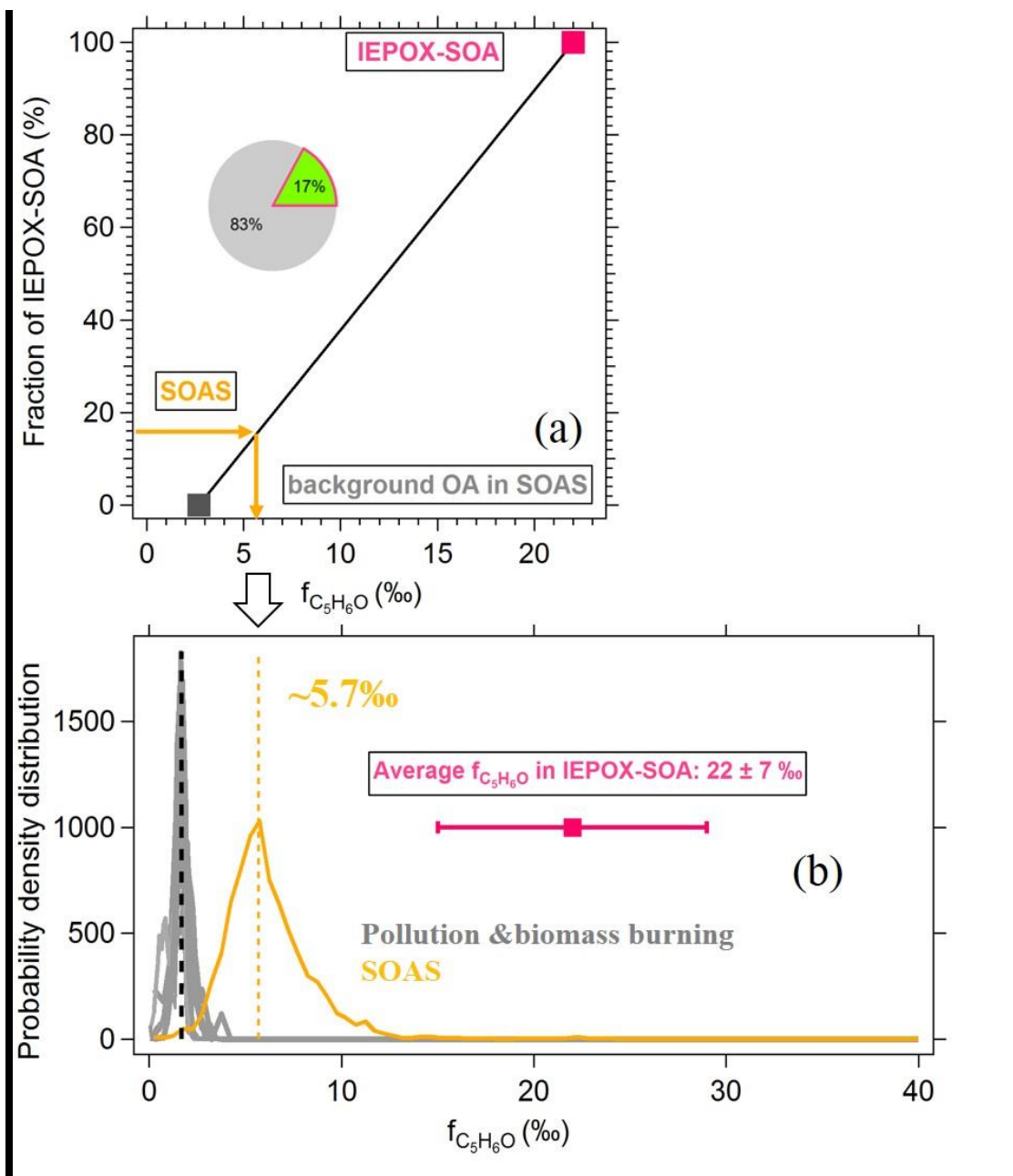
39

40
41



42
43 **Figure S6.** Time series of OA mass concentration, and of tracers for IEPOX-SOA ($f_{C_5H_6O}$) and
44 biomass-burning ($f_{C_2H_4O_2}$, m/z 60.0211) compared to their respective backgrounds on the
45 research flight on Aug 26, 2013 during the SEAC4RS campaign. The biomass-burning tracer
46 indicates extensive fire influence during this period, while the IEPOX-SOA tracer stays at
47 background levels across widely varying OA concentrations.

48



49

50 **Figure S7.** Schematic of the estimation method of IEPOX-SOA based on ambient $f_{C_5H_6O}$. (a)

51 Fraction of IEPOX-SOA in total OA vs ambient $f_{C_5H_6O}^{OA}$ (b) probability distribution of $f_{C_5H_6O}^{OA}$ in

52 SOAS and in background studies. The average background of $f_{C_5H_6O}^{OA}$ from SOAS-CTR should be

53 between the $f_{C_5H_6O}$ from urban and biomass burning emissions (~ 1.7 ‰) and $f_{C_5H_6O}$ strongly

54 influenced by monoterpene emissions, which we can use 3.7‰ from Rocky Mountain site as

55 representative value. An average $f_{C_5H_6O}^{OA}$ value of 2.7‰ was used here for the background $f_{C_5H_6O}^{OA}$

56 for SOAS-CTR. $f_{C_5H_6O}$ in IEPOX-SOA_{PMF} is 22‰. Two values corresponding to 0% and 100%

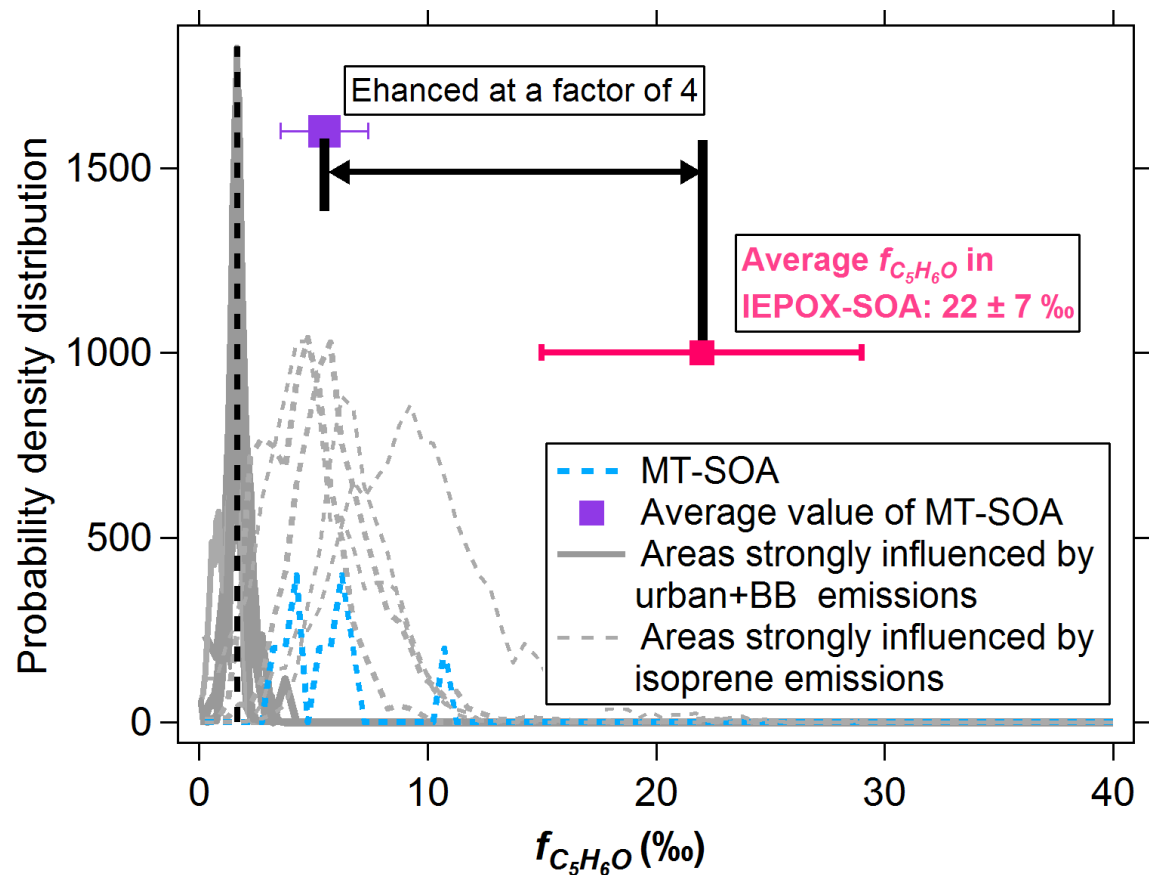
57 IEPOX-SOA in total OA, are shown as two square points shown in Fig. S5a. If we assume the

58 air containing these two types of OA are mixed with each other, then we can draw a line between

59 these two points in Fig. S5a. Ambient $f_{C_5H_6O}^{OA}$ partially contributed by IEPOX-SOA should vary
60 along this line. Take SOAS as an example, 17% of OA in SOAS was composed by IEPOX-SOA,
61 then it corresponds to an expected average $f_{C_5H_6O}^{OA}$ of $\sim 5.7\%$, which is consistent with what was
62 observed (Fig. S5b). The peak of the probability distribution of $f_{C_5H_6O}^{OA}$ in SOAS is around 5.7%.

63

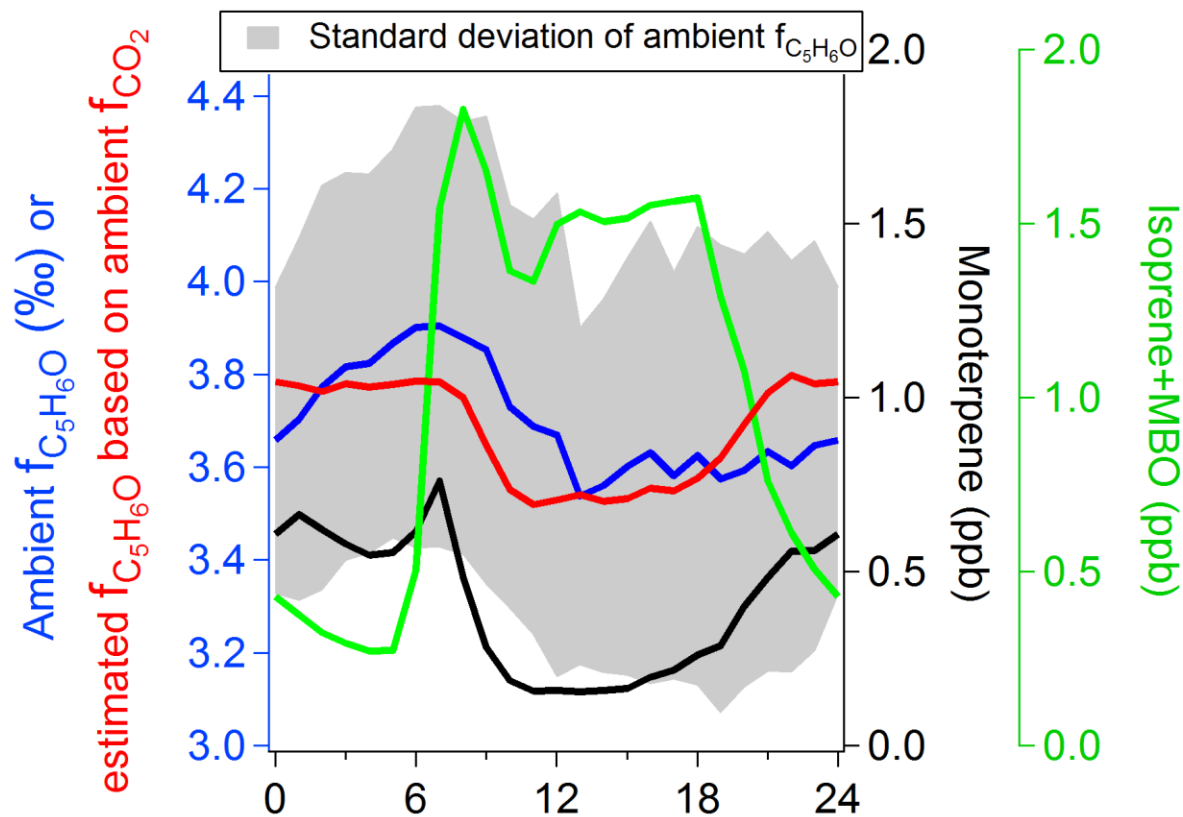
64



65

66 **Figure S8** Comparison between $f_{C_5H_6O}^{MT-SOA}$ and $f_{C_5H_6O}^{IEPOX-SOA}$, $f_{C_5H_6O}^{OA}$ from areas strongly
 67 influenced by urban + biomass burning and isoprene emissions are also shown.

68



69

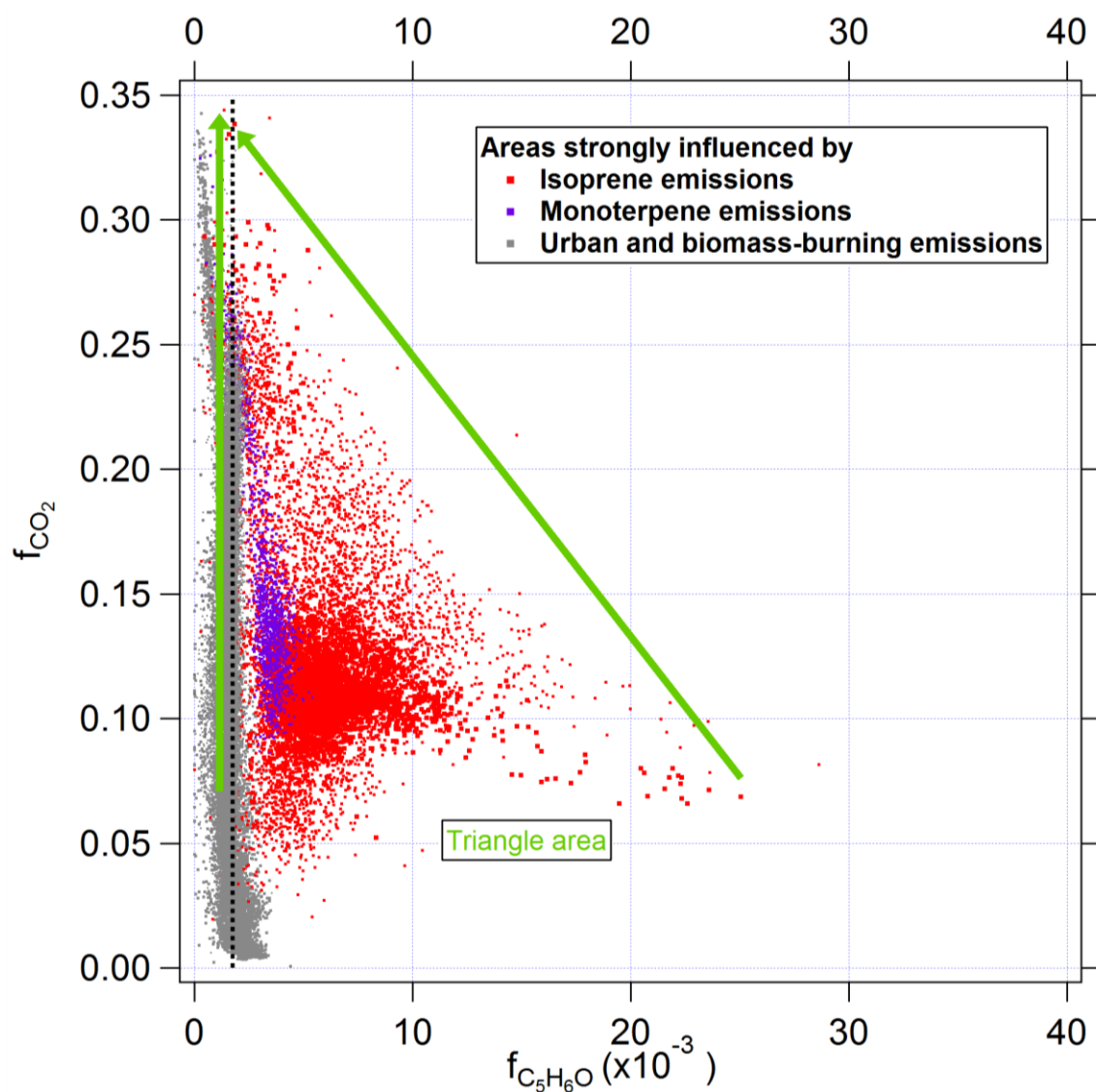
70 **Figure S9.** Diurnal variation of ambient $f_{C_5H_6O}^{OA}$ at the Manitou Forest pine forest site in the
 71 Rocky Mountains during the BEACHON-RoMBAS 2011 field study, together with diurnal
 72 variations of estimated $f_{C_5H_6O}^{OA}$ from $f_{CO_2}^{OA}$ based on regression results between $f_{C_5H_6O}^{OA}$ and $f_{CO_2}^{OA}$
 73 (ambient+Oxidation flow reactor) in this study. The diurnal variation of monoterpene and
 74 isoprene+MBO are also shown.

75

76

77

78



79

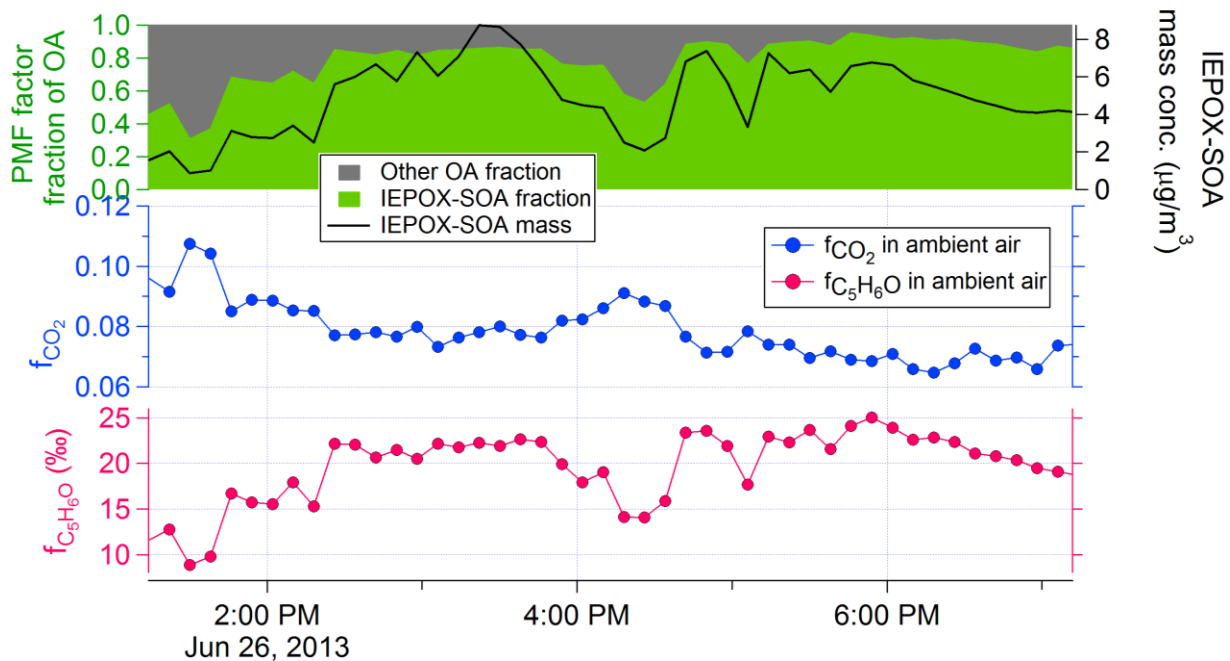
80 **Figure S10.** Scatter plot between $f_{CO_2}^{OA}$ and $f_{C_5H_6O}^{OA}$ for all the ambient OA dataset. Green arrows
 81 are added to guide the eye.

82

83

84

85

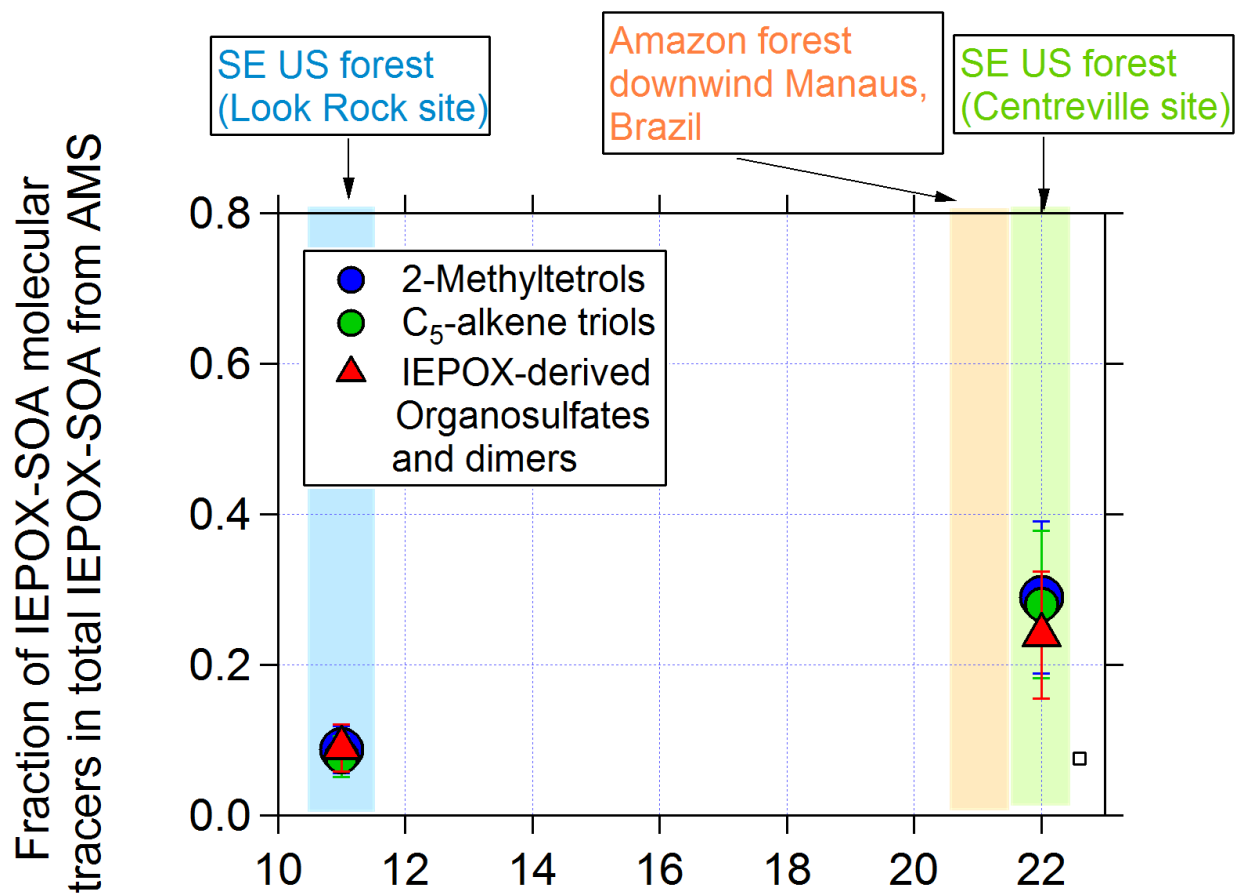


86

87 **Figure S11.** Time series of ambient $f_{C_5H_6O}^{OA}$, $f_{CO_2}^{OA}$, and IEPOX-SOA mass concentrations, together
 88 with the IEPOX-SOA fraction of OA during the SOAS-CTR campaign in a SE US forest. During
 89 this period, high sulfate and IEPOX-SOA mass concentrations and mass fractions are observed.

90

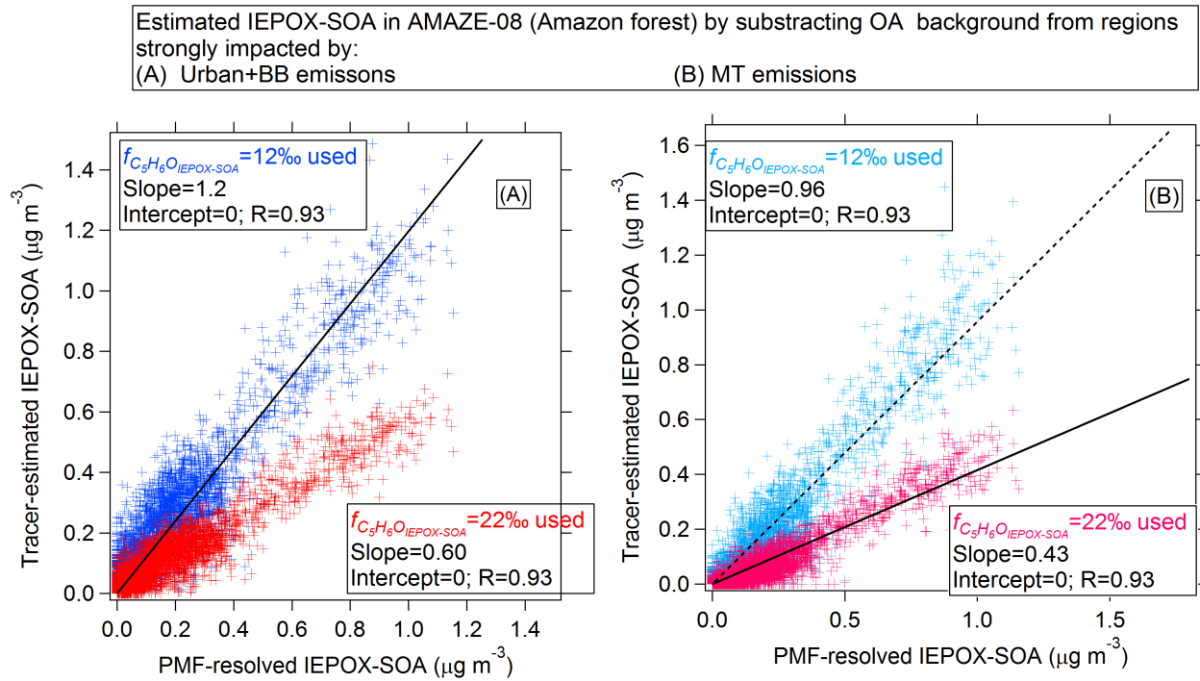
91



92

93 **Figure S12** Scatter plot between different IEPOX-SOA molecular tracers (Methyltetrol, C5-
 94 alkene triols and IEPOX-derived organosulfates and their dimers) vs IEPOX-SOAPMF and f_{82} in
 95 IEPOX-SOA

96



98

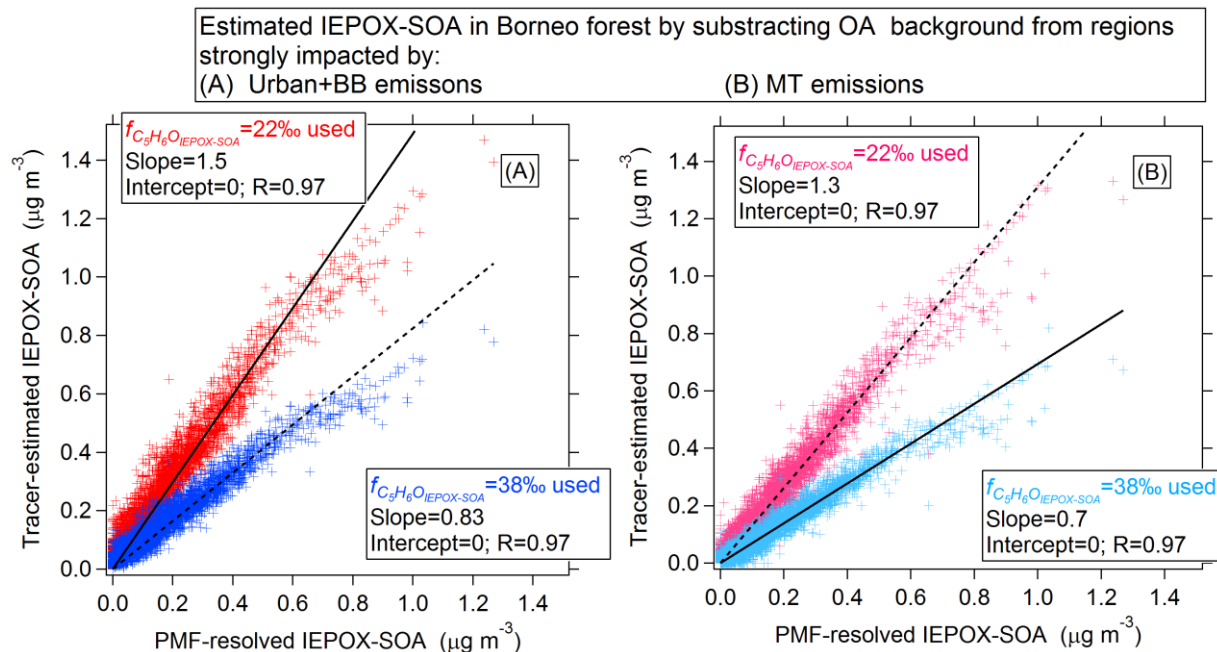
99 **Figure S13.** Scatter plot between tracer-estimated IEPOX-SOA and IEPOX-SOA_{PMF} at a pristine
 100 Amazon forest site (AMAZE-08). The tracer-based IEPOX-SOA was estimated using OA
 101 background from regions strongly influenced by (A) urban and biomass-burning emissions and
 102 (B) monoterpene emissions. In each plot, we used two $f_{\text{C}_5\text{H}_6\text{O}}^{\text{IEPOX-SOA}}$, from the average IEPOX-
 103 SOA_{PMF} ($f_{\text{C}_5\text{H}_6\text{O}}^{\text{IEPOX-SOA}}=22\text{‰}$) and from the IEPOX-SOA_{PMF} in Amazon forest study
 104 ($f_{\text{C}_5\text{H}_6\text{O}}^{\text{IEPOX-SOA}}=12\text{‰}$).

105

106

107

108



109

110 **Figure S14** Scatter plot between estimated IEPOX-SOA and IEPOX-SOA_{PMF} at a Borneo forest
 111 site. The tracer-based IEPOX-SOA was estimated using OA background from regions strongly
 112 influenced by (A) urban and biomass-burning emissions and (B) monoterpene emissions. In each
 113 plot, we used two $f_{C_5H_6O}^{IEPOX-SOA}$, from the average IEPOX-SOA_{PMF} ($f_{C_5H_6O}^{IEPOX-SOA}=22\%$) and from
 114 the IEPOX-SOA_{PMF} in Borneo forest study ($f_{C_5H_6O}^{IEPOX-SOA}=38\%$).

115

116 1.1 Bounds for using the IEPOX-SOA estimation method

117 In theory, our method can easily produce an estimate of “IEPOX-SOA” from an AMS
118 dataset, but the errors could be substantial in some cases. The guidelines below are meant to limit
119 the errors when applying this method:

- 120 1) We first recommend making the scatter plot of $f_{CO_2}^{OA}$ and $f_{C_5H_6O}^{OA}$ and then compare it to
121 Fig. 5 in this study to help evaluate the possible presence of IEPOX-SOA.
- 122 2) For datasets where an important influence of MT-SOA is suspected: if all the $f_{C_5H_6O}^{OA}$ in
123 total OA are $\sim 3.1\%$ or lower within measurement noise, the estimated IEPOX-SOA will
124 show negative and positive values scattered around zero, indicating negligible IEPOX-
125 SOA in the dataset. A similar conclusion can be reached for urban or BB-dominated
126 locations when $f_{C_5H_6O}^{OA} \sim 1.7\%$ or lower for most data points.
- 127 3) When the scatter plot between $f_{CO_2}^{OA}$ and $f_{C_5H_6O}^{OA}$ shows obvious enhanced $f_{C_5H_6O}^{OA}$ above the
128 most-relevant background value, users can easily use the tracer-based method to estimate
129 the IEPOX-SOA mass concentration. If the source of the background OA is not known,
130 we suggest using both background corrections and reporting the range of results.
- 131 4) Cases intermediate between No. 2 and 3 above, i.e. when $f_{C_5H_6O}^{OA}$ is only slightly above the
132 relevant background level will have the largest relative uncertainty. In this case we
133 recommend applying the method and evaluating the results carefully, as exemplified for
134 the Rocky Mountain dataset in this paper (section 3.5). E.g. diurnal variations of $f_{C_5H_6O}^{OA}$
135 and SOA precursors (e.g., isoprene and monoterpene), together with diurnal variation of
136 estimated IEPOX-SOA, provide useful indicators about whether the results are
137 meaningful. For cases in which the fraction of IEPOX-SOA in total OA is relatively low
138 (e.g., $< 5\%$) and the fraction of MT-SOA in total OA is high (e.g., $> 50\%$), the uncertainty
139 of the IEPOX-SOA estimate will be very high. For this type of situation the full PMF
140 method may be required.

141 Besides ease of use, another advantage of the tracer-based estimation method is that it can
142 be used to quantify IEPOX-SOA based on brief periods of elevated concentrations, e.g. as often
143 encountered in aircraft studies. In those cases it may be difficult for PMF to resolve an IEPOX-
144 SOA factor, but no such limitation applies to this estimation method.

145 1.2 Uncertainties of IEPOX-SOA estimation method.

146 To estimate the accuracy of our IEPOX-SOA tracer-based estimation method, we used this
147 method to estimate IEPOX-SOA from another two ambient datasets with the lowest and highest
148 $f_{C_5H_6O}^{IEPOX-SOA}$ in PMF-resolved IEPOX-SOA ($f_{C_5H_6O}^{IEPOX-SOA, PMF}$) among all the studies in this paper.
149 The lowest value is from a dataset in the pristine Amazon forest (AMAZE-08) where
150 $f_{C_5H_6O}^{IEPOX-SOA} = 12\%$ (Chen et al., 2015) and the highest value from a dataset in a Borneo forest
151 with $f_{C_5H_6O}^{IEPOX-SOA} = 38\%$ (Robinson et al., 2011). Since the $f_{C_5H_6O}^{IEPOX-SOA}$ values in these two
152 datasets are the two farthest from the average $f_{C_5H_6O}^{IEPOX-SOA} (22 \pm 7\%)$, the estimation method

153 results from these two datasets represent the worst case scenarios for all datasets published so
154 far.

155 The estimation results from both datasets are shown in Fig. S13 and Fig. S14. Both of the
156 background OA corrections for areas strongly influenced by urban+BB emissions and by
157 monoterpene emissions are used.

158 Overall, all variants of the estimated IEPOX-SOA correlate well with IEPOX-SOA_{PMF} (all
159 $R \geq 0.93$). When average $f_{C_5H_6O}^{IEPOX-SOA} = 22\%$ is used, the slope between estimated IEPOX-SOA
160 vs IEPOX-SOA_{PMF} is between 0.43-1.5, i.e. within a factor of 2.2. When the actual $f_{C_5H_6O}^{IEPOX-SOA}$ in
161 each dataset is used, the slope between estimated IEPOX-SOA vs IEPOX-SOA_{PMF} is in a range
162 of 0.7-1.2, i.e. within 30%.

163

164

165

166 **References**

167 Aiken, A. C., Salcedo, D., Cubison, M. J., Huffman, J. A., DeCarlo, P. F., Ulbrich, I. M.,
 168 Docherty, K. S., Sueper, D., Kimmel, J. R., Worsnop, D. R., Trimborn, A., Northway,
 169 M., Stone, E. A., Schauer, J. J., Volkamer, R. M., Fortner, E., de Foy, B., Wang, J.,
 170 Laskin, A., Shutthanandan, V., Zheng, J., Zhang, R., Gaffney, J., Marley, N. A., Paredes-
 171 Miranda, G., Arnott, W. P., Molina, L. T., Sosa, G., and Jimenez, J. L.: Mexico City
 172 aerosol analysis during MILAGRO using high resolution aerosol mass spectrometry at
 173 the urban supersite (T0) - Part 1: Fine particle composition and organic source
 174 apportionment, *Atmos Chem Phys*, 9, 6633-6653, 2009.

175 Canagaratna, M. R., Jimenez, J. L., Kroll, J. H., Chen, Q., Kessler, S. H., Massoli, P.,
 176 Hildebrandt Ruiz, L., Fortner, E., Williams, L. R., Wilson, K. R., Surratt, J. D., Donahue,
 177 N. M., Jayne, J. T., and Worsnop, D. R.: Elemental ratio measurements of organic
 178 compounds using aerosol mass spectrometry: characterization, improved calibration, and
 179 implications, *Atmos. Chem. Phys.*, 15, 253-272, 10.5194/acp-15-253-2015, 2015.

180 Chen, Q., Farmer, D. K., Rizzo, L. V., Pauliquevis, T., Kuwata, M., Karl, T. G., Guenther, A.,
 181 Allan, J. D., Coe, H., Andreae, M. O., Pöschl, U., Jimenez, J. L., Artaxo, P., and Martin,
 182 S. T.: Submicron particle mass concentrations and sources in the Amazonian wet season
 183 (AMAZE-08), *Atmos. Chem. Phys.*, 15, 3687-3701, 10.5194/acp-15-3687-2015, 2015.

184 Chhabra, P. S., Flagan, R. C., and Seinfeld, J. H.: Elemental analysis of chamber organic aerosol
 185 using an aerodyne high-resolution aerosol mass spectrometer, *Atmos. Chem. Phys.*, 10,
 186 4111-4131, 10.5194/acp-10-4111-2010, 2010.

187 Crippa, M., El Haddad, I., Slowik, J. G., DeCarlo, P. F., Mohr, C., Heringa, M. F., Chirico, R.,
 188 Marchand, N., Sciare, J., Baltensperger, U., and Prévôt, A. S. H.: Identification of marine
 189 and continental aerosol sources in Paris using high resolution aerosol mass spectrometry,
 190 *Journal of Geophysical Research: Atmospheres*, 118, 1950-1963, doi:
 191 10.1002/jgrd.50151, 2013.

192 Docherty, K. S., Aiken, A. C., Huffman, J. A., Ulbrich, I. M., DeCarlo, P. F., Sueper, D.,
 193 Worsnop, D. R., Snyder, D. C., Peltier, R. E., Weber, R. J., Grover, B. D., Eatough, D. J.,
 194 Williams, B. J., Goldstein, A. H., Ziemann, P. J., and Jimenez, J. L.: The 2005 Study of
 195 Organic Aerosols at Riverside (SOAR-1): instrumental intercomparisons and fine particle
 196 composition, *Atmos. Chem. Phys.*, 11, 12387-12420, 10.5194/acp-11-12387-2011, 2011.

197 Dunlea, E. J., DeCarlo, P. F., Aiken, A. C., Kimmel, J. R., Peltier, R. E., Weber, R. J.,
 198 Tomlinson, J., Collins, D. R., Shinozuka, Y., McNaughton, C. S., Howell, S. G., Clarke,
 199 A. D., Emmons, L. K., Apel, E. C., Pfister, G. G., van Donkelaar, A., Martin, R. V.,
 200 Millet, D. B., Heald, C. L., and Jimenez, J. L.: Evolution of Asian aerosols during
 201 transpacific transport in INTEX-B, *Atmos Chem Phys*, 9, 7257-7287, 2009.

202 Robinson, N. H., Hamilton, J. F., Allan, J. D., Langford, B., Oram, D. E., Chen, Q., Docherty,
 203 K., Farmer, D. K., Jimenez, J. L., Ward, M. W., Hewitt, C. N., Barley, M. H., Jenkin, M.
 204 E., Rickard, A. R., Martin, S. T., McFiggans, G., and Coe, H.: Evidence for a significant
 205 proportion of Secondary Organic Aerosol from isoprene above a maritime tropical forest,
 206 *Atmos. Chem. Phys.*, 11, 1039-1050, 10.5194/acp-11-1039-2011, 2011.

207 Setyan, A., Zhang, Q., Merkel, M., Knighton, W. B., Sun, Y., Song, C., Shilling, J. E., Onasch,
 208 T. B., Herndon, S. C., Worsnop, D. R., Fast, J. D., Zaveri, R. A., Berg, L. K.,
 209 Wiedensohler, A., Flowers, B. A., Dubey, M. K., and Subramanian, R.: Characterization
 210 of submicron particles influenced by mixed biogenic and anthropogenic emissions using

211 high-resolution aerosol mass spectrometry: results from CARES, *Atmos. Chem. Phys.*,
212 12, 8131-8156, 10.5194/acp-12-8131-2012, 2012.
213 Ulbrich, I. M., Canagaratna, M. R., Zhang, Q., Worsnop, D. R., and Jimenez, J. L.: Interpretation
214 of organic components from Positive Matrix Factorization of aerosol mass spectrometric
215 data, *Atmos Chem Phys*, 9, 2891-2918, 2009.

216

217